Next Generation Vehicle Positioning Techniques for GPS-Degraded Environments to Support Vehicle Safety and Automation Systems

FHWA BAA DTFH61-09-R-00004

EXPLORATORY ADVANCED RESEARCH PROGRAM

Auburn University

Sarnoff Corporation

The Pennsylvania State University

Kapsch TrafficCom Inc.

NAVTEQ North America LLC

Quarterly Report 4

July – Sept 2010

Table of Contents

1. SCOPE **3**

1.1 SARNOFF CORPORATION CONTRIBUTION 3
1.2 THE PENNSYLVANIA STATE UNIVERSITY CONTRIBUTION 4
1.3 KAPSCH TRAFFICCOM INC. CONTRIBUTION 4

2. CURRENT PROGRESS **5**

2.1 SARNOFF PROGRESS 5
2.1.1 Components *5*
2.1.2 Design *5*
2.1.3 Installation *8*
2.1.4 Data Collection *8*
2.2 PENN STATE PROGRESS 9
2.2.1 Real-time Implementation *9*
2.2.2 Effect of Terrain and Algorithm Sampling Rate on Localization Accuracy *9*
2.2.3 Field testing of real-time implementation *12*
2.2.4 Multiple Model Estimation for Road Network Implementation *12*
2.3 KAPSCH TRAFFICCOM INC. PROGRESS 12
2.3.1 Initial Range Testing *12*
2.4 AUBURN CURRENT PROGRESS 14

3. FUTURE WORK **14**

3.1 SARNOFF FUTURE WORK 14
3.1.1 Analysis of Data *14*
3.1.2 Use of GPS packets *14*
3.1.3 Delivery of Clevo laptop *14*
3.2 PENN STATE FUTURE WORK 15
3.3 KAPSCH FUTURE WORK 15
3.4 AUBURN FUTURE WORK 15

REFERENCES **15**

GANTT CHART **17**

1. Scope

In an open environment, GPS provides a good estimation of vehicle position. Numerous improvements over the basic GPS framework have provided accuracies in the centimeter range. However, blockages of the GPS signal create significant problems for the positioning solution. In so-called "urban canyons", GPS signals are blocked by the presence of tall buildings. Similarly, heavy foliage in forests can block line-of-sight to the satellites. Because of these problems, a broader approach is needed that does not rely exclusively on GPS. This project takes into account three key technology areas which have each been individually shown to improve positioning solutions where GPS is not available or is hampered in a shadowed environment. First, terrain-based localization can be readily used to find the vehicle's absolute longitudinal position within a pre-mapped highway segment – compensating for drift which occurs in dead-reckoning system in long longitudinal stretches of road. Secondly, visual odometry keys upon visual landmarks at a detailed level to correlate position to a (visually) premapped road segment to find vehicle position along the roadway. Both of these preceding techniques rely on foreknowledge of road features – in essence, a feature-enhanced version of a digital map. This becomes feasible in the "connected vehicle" future, in which tomorrow's vehicles have access to quantities of data orders of magnitude greater than today's cars, as well as the ability to share data at high data rates. The third technology approach relies on radio frequency (RF) ranging based on DSRC radio technology. In addition to pure RF ranging with no GPS signals, information from RF ranging can be combined with GPS range measurements (which may be inadequate on their own) to generate a useful position. Based on testing and characterization of these technologies individually in a test track environment, Auburn will define a combined Integrated Positioning System (IPS) for degraded GPS environments, which will also incorporate ongoing FHWA EAR work at Auburn in fusion of GPS and on-board sensors. This integrated approach will blend the strengths of each technique for greater robustness and precision overall. This research is expected to be a major step forward towards exceptionally precise and reliable positioning by taking advantage of long-term trends in on-board computing, connected vehicles, and data sharing.

1.1 Sarnoff Corporation Contribution

The scope of Sarnoff's work under Year One of this project is the evaluation of their Visual Aided Navigation System for providing highly accurate positioning for vehicles. As such there are 3 major tasks:

(1) Evaluate and provide a survey of Sarnoff's existing Visual Navigation results

(2) Integrate Visual Navigation system on Auburn Engineering's G35 vehicle test platform and collect test data using the integrated system.

(3) Process and analyze the data from the tests and evaluate the performance and recommend any improvements and optimizations.

1.2 The Pennsylvania State University Contribution

For sake of clarity and coherence, the scope of Penn State's contribution to the project, as discussed in previous quarterly reports, is reproduced here. The primary objectives under Penn State's purview are:

(1) Developing the proven particle filter approach so that it can be used for localization with commercial-grade sensors, rather than defense-grade sensors,
(2) Modifying and optimizing the particle filter algorithm, and exploring alternative approaches, so that localization can take place online (in real-time) rather than offline, and
(3) Modifying and optimizing the algorithms as well as terrain map representation, so that the localization algorithms work over a large network of roads, rather than a small section of a single road alone.

Following up from previous quarterly reports, as part of Task (2), Penn State has completed the offline testing of the Simulink model developed for real-time implementation. The model is now being incorporated into the QuaRC/Simulink architecture for field testing. Work on Task (3) is progressing with review of prevalent multiple model estimation techniques which will be used for vehicle position tracking on a large road network.

1.3 Kapsch TrafficCom Inc. Contribution

Kapsch will investigate the accuracy of close proximity calculations available from the 5.9 GHz DSRC communications channel. A great deal of information related to positioning can be inferred from the DSRC communications channel. Basic calculations may provide a location region achieved through the channel ranging calculations to more precise lane based proximity determinations through advanced analysis of the communications channel. Kapsch will research a combination of both approaches through available data defined in the IEEE 802.11p standard for 5.9 GHz communication and through scientific Radio Frequency (RF) analysis.

Kapsch will support Auburn for the characterization of the ability to utilize the 5.9 GHz DSRC communication channel for next generation non-GPS localization services. The Received Signal Strength Indication (RSSI) in-conjunction with other aspects of the DSRC communications channel will be analyzed and a method developed for signal ranging. Kapsch does not believe RSSI ranging techniques will fully meet the desired localization needs. Year 2 will yield more advanced algorithms and DSRC equipment capable of providing lane level localization from the DSRC communications channel. This task includes the following sub-tasks:

(1) System Engineering and Deployment of DSRC Infrastructure at the Auburn Test Track
(2) Lab testing of DSRC signal ranging solution
(3) On-site testing of DSRC signal ranging solution
(4) Analysis of DSRC signal ranging test results

2. Current Progress

2.1 Sarnoff Progress

The visual navigation sensor package was delivered to Auburn University and installed on the test vehicle on 10/3/2010.

2.1.1 Components

The components used in the sensor package include cameras, IMU, Ethernet hub, trigger circuit, cabling, and laptop computer.

- Cameras (4) - Allied Vision Prosilica GC1380
  - GigaBit Ethernet interface
  - 640x480 (after 2x2 binning)
  - 30 fps,
  - Sony ICX285 CCD, monochrome
- Lenses (4) - Kowa LM6JC
  - 6.0 mm/F1.4
- IMU (1) – CloudCap Crista
  - 100 Hz operation
  - 10x oversampling
- Ethernet hub (1) – Netgear GS105NA
  - 5 RJ45 ports
  - Jumbo frame support to 9720 bytes
- Cabling and connectors
  - Weather proof RJ45 connectors
  - Shielded CAT6 cable
  - Mil-style 10 pin connectors
- Computer (1) – AVA Direct Clevo D900F
  - Intel quadcore i7, 3.33 GHz

2.1.2 Design

The sensor payload was designed towards several criteria. The package consists of a front camera box, a rear camera box, and a power and data breakout box. The front and rear boxes need to be rigidly connected and it must be possible to remove the boxes without detaching them from this rigid coupling. The boxes must be positioned on the vehicle such that they are not occluded by, nor do they occlude, the existing sensors, racks, and the vehicle itself. In addition, the boxes must be weather proof and robust to vibration and heat variation.

The figure below shows the Sarnoff camera setup. The front camera enclosure shows two cameras and an IMU. Various signals are sent to the back camera enclosure, where two cameras and a gigabit hub can be seen. The power of the system comes out of a breakout box, and the laptop is connected to the remaining signals.

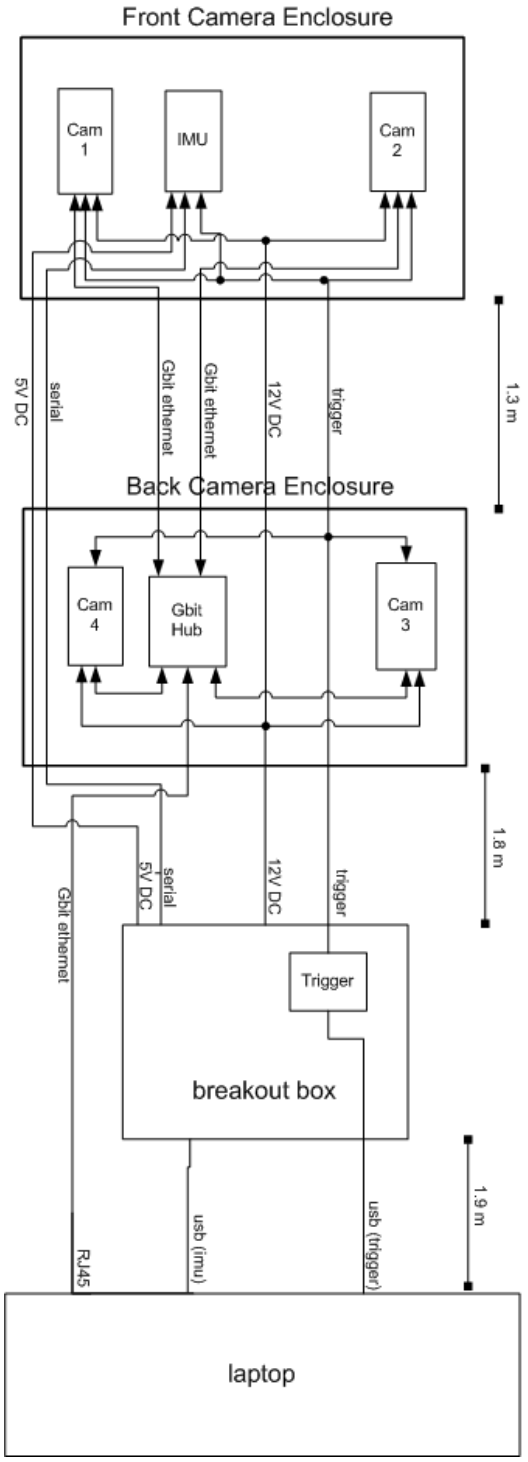

Figure 1: Wiring diagram and physical layout of components in the visual navigation sensor package.

The front camera enclosure sits above the front windshield, on the driver's side. The back camera enclosure sits above the rear windshield, on the driver's side. The power breakout box is mounted in the trunk. The laptop can be placed in the front passenger seat.

The CAD model can be seen with an isometric view. Two bars extend parallel. A center bar joins the two bars. On the front bar, two antennas can be seen on either end, with the LiDAR visible at the middle of the front bar. The rear view bar has a Septentrio antenna at its center. Near the front on the middle bar is another Sepentrio antenna. Near the back on the middle bar is an antenna. The Sarnoff mount can be seen to the right of the middle bar. The mount extends from the front bar to the back bar with a double layer of 80x20. Three more bars keep the two bars combined at an equal distance. The cameras hang on either end of the Sarnoff bars and are pointed to the back and the front of the vehicle.

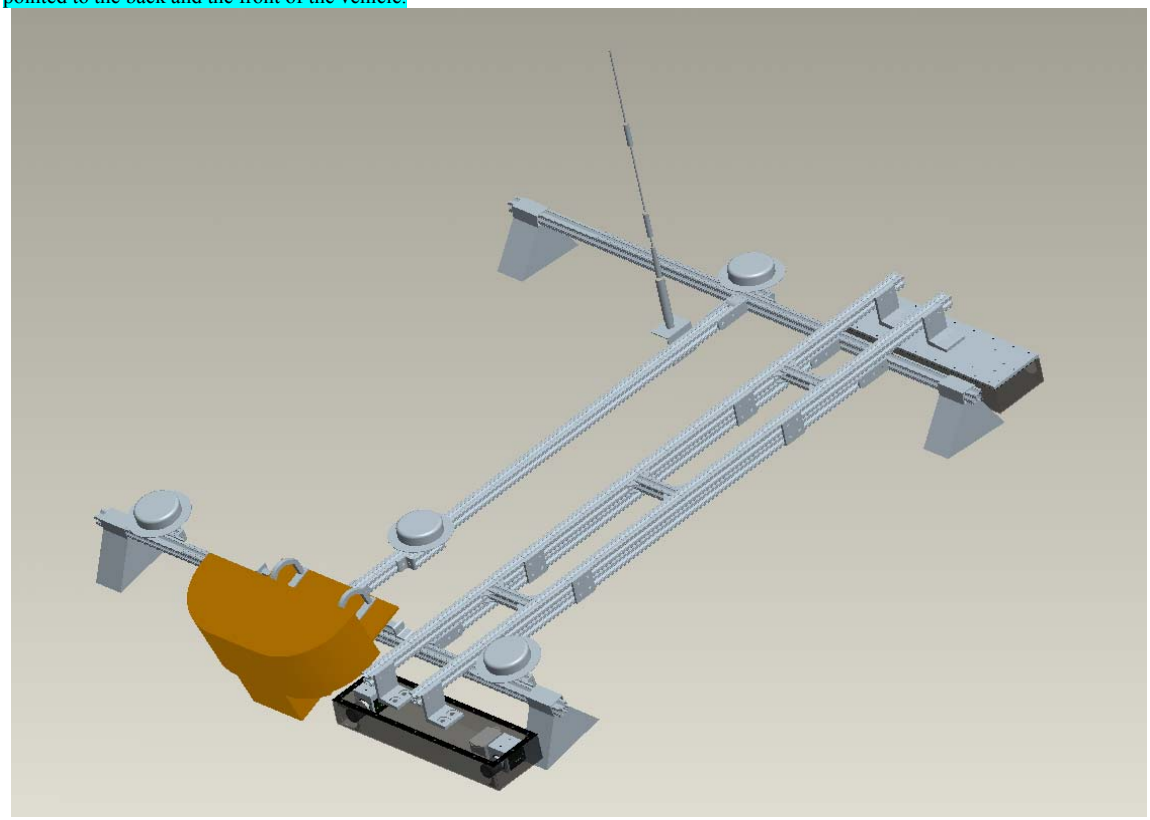

Figure 2: CAD model of the front and rear camera enclosures, shown in relation to the existing roof rack, antennas, and IBEO lidar on the test vehicle.

The figure below shows the CAD model of the front view of the sensor package. The LiDAR dominates the front center of the image. A piece of 80x20 bar stretches to either side of the image. Two antennas for the Septentrio are visible at the ends of the bar. The camera is visible as hanging down the right side of the bar below the antenna. Above the LiDAR, an antenna is visible from the back of the vehicle.

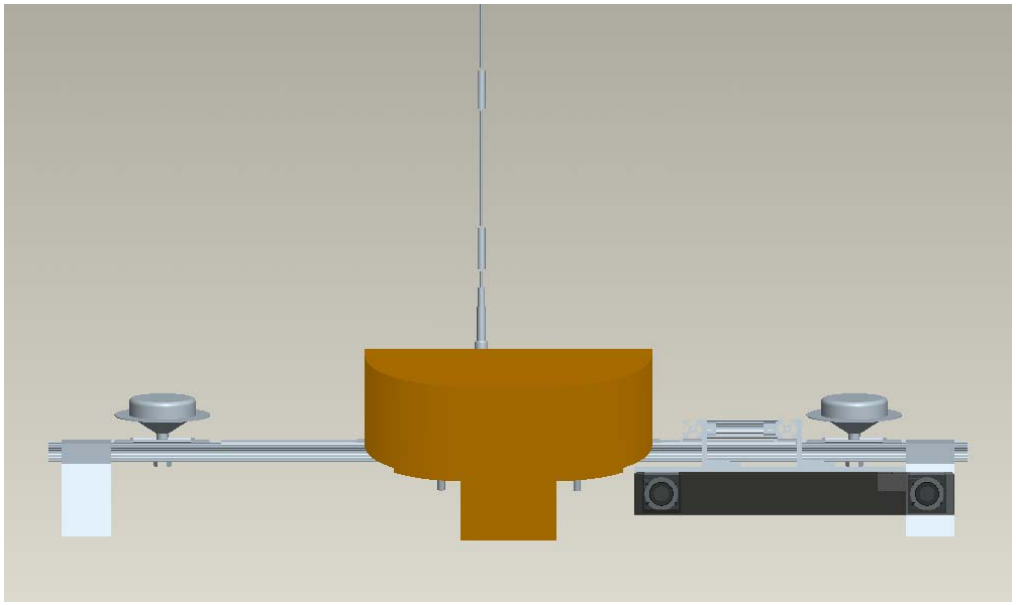

Figure 3: Front view of sensor package.

2.1.3 Installation

The sensor payload installation on the Infiniti test vehicle was begun on 10/3/2010 and finished on 10/4/2010. The existing T-slot bars needed to be replaced with longer bars (provided by Auburn University) at time of installation because the connectors to the rear sensor box were obstructed by the rear windshield. 5V and 12V power was supplied by the Auburn vehicle's power supply panel.

A full calibration was performed at time of installation. Intrinsic model parameters were calculated for each camera using the Bouguet calibration method. Extrinsic parameters (relative position and orientation in 6 degrees of freedom) were calculated between the cameras in the front stereo pair, the cameras in the back stereo pair, the front left camera and the IMU, the back left camera and the IMU, and the front left camera and the vehicle center. The extrinsic calibration between the back left camera and the IMU did not converge to a valid solution during the trip to Auburn University, so raw data was collected (video and IMU data) and the calibration will be recalculated by Sarnoff.

2.1.4 Data Collection

Once installed, the visual navigation sensor package was tested on the Auburn University test track. Data (video, IMU data, and GPS positions) was recorded in several different modes (2 cameras only, 4 cameras, 15 fps, and 30 fps) and in different driving modes (varying speed and lighting conditions). In addition, connectivity between the Sarnoff computer and the Auburn vehicle computer was tested by sending position and orientation updates over TCP/IP.

2.2 Penn State Progress

2.2.1 Real-time Implementation

Task (2) entails the development of a real-time implementation of the localization algorithm. It was stated in the previous quarterly report that the Simulink diagram was still undergoing testing in the offline environment to verify its efficacy. The testing phase is now complete and the diagram is being tested in the field at Penn State. The offline testing has shown that the UKF algorithm can be effectively used for vehicle position tracking with a variety of sensors having different characteristics. Specifically, it has been shown through simulation that meter-level accuracy can be achieved even with commercial-grade sensors such as the XBOW 440. Figure 4 depicts the tracking error for sample simulation wherein a simulated XBOW 440 was used for tracking the vehicle position on a highway.

The figure below shows the tracking error using simulated XBOW data and data collected on Highway 322. The tracking error increases from 0 m to about 0.75 m after 10 seconds. At around 20 seconds, the tracking error increases to one meter in error. The error stays fairly constant until 80s, at which time the error increases slightly to 1.25m. Throughout the graph, the error spikes to a lower error by about .4 m every few seconds.

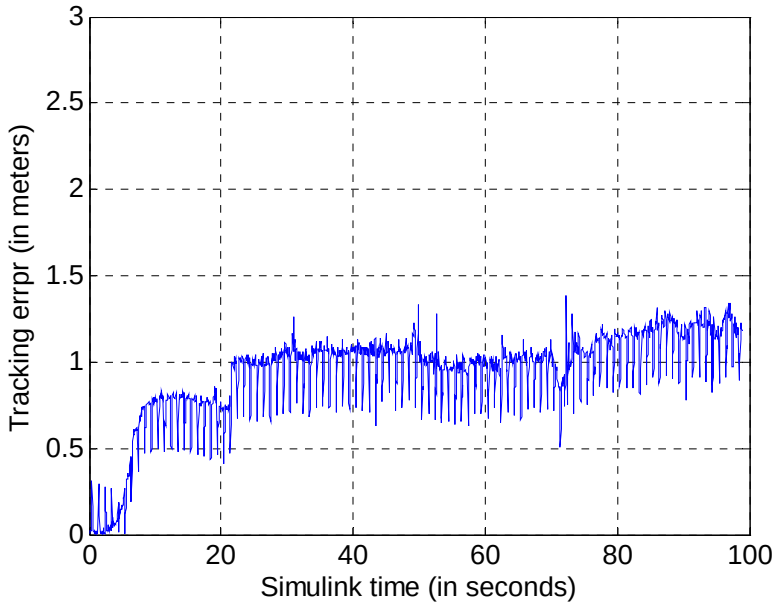

Figure 4: Tracking error using simulated XBOW 440 and data collected on Highway 322.

2.2.2 Effect of Terrain and Algorithm Sampling Rate on Localization Accuracy

While testing the SPKF algorithm, it was observed that the mean accuracy of the SPKF varies significantly based on two factors, viz.

(a) Terrain, i.e. the type of road over which the vehicle is traveling. For example, localization accuracy on a highway is different from that on a secondary or rural road, with all other factors remaining unchanged.

(b) Sampling rate of the SPKF algorithm, i.e. the distance after which the filter is updated using new terrain measurements.

It was found that the SPKF performs much better on secondary roads as compared to highways. This finding conforms to intuition, since it is expected that a road with large variations in terrain provides more features and information, and hence a better tracking ability, as compared to a completely flat road with no variations in terrain. As is evident from Figure 5, the terrain variations are more pronounced on secondary roads as compared to highways.

It was also observed that the mean tracking error output was smaller for larger sampling intervals, e.g. the distance traveled by a vehicle before the SPKF is updated using new measurements. Figure 6 indicates the reduction in mean error as the sampling interval increases, for both highways and secondary roadways.

The trends observed in Figure 6 are a consequence of the sensor fusion taking place in the SPKF algorithm. Specifically, incoming data from the encoders, which represent the motion model, are being fused with data from the inertial measurement unit, which represents the measurement model. At short distances (i.e. small sampling rates), the encoder dominates since there is no appreciable difference in terrain. As a consequence, IMU measurements have little contribution towards providing a rectifying update to the position estimate. However, at longer distances (i.e. large sampling rates), the encoder error accumulates, but the terrain also changes by a significant amount which allows larger IMU corrections of the position estimate in the subsequent "correction" or measurement update step. In addition, Figure 6 also indicates the difference in localization accuracy of the algorithm on different roadways. To state it more clearly, it may be observed that the mean longitudinal position error on secondary roads (Rock Rd) is much smaller than the mean error on highways (Highway 322).

The graph below shows the pitch in degrees for Rock Road (a secondary road) and Highway 322. The Rock Road pitch changes drastically from about -2 degrees at the start to 3 degrees after around 175m. The pitch for Rock Road alternates about 2 degrees until 400 meters, at which point the pitch falls to -1.5 degrees. Once more, the pitch fluctuates about 2 degrees until 1000m, where the pitch approaches 0 degrees. The Highway 322 pitch, however, begins at -2 degrees, changes to about -1.5 degrees after about 100 meters, and slightly fluctuates until 550 meters, at which time there is a linear increase in pitch to 800 meters to slightly more than 1 degree. The pitch again stays fairly constant until 1000m and is quickly followed by a gradual decrease to 0 degrees to the end of the test run.

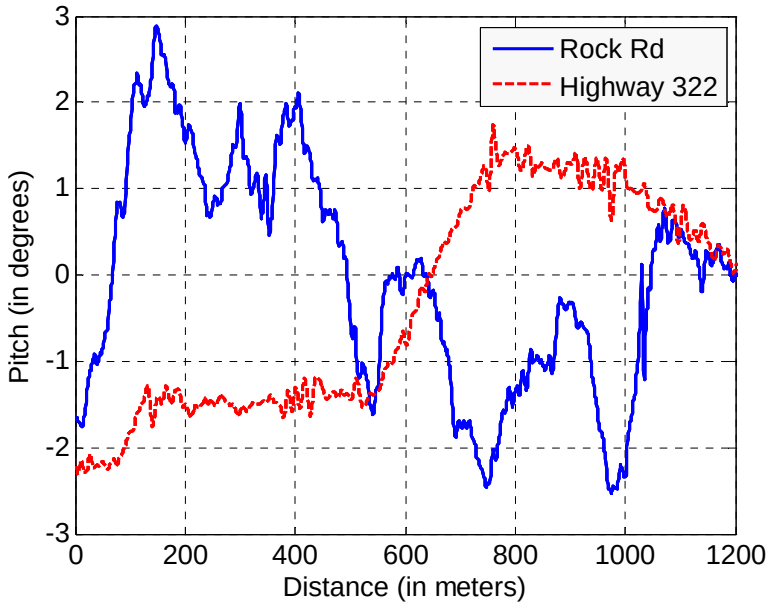

Figure 5: Pitch variations on Rock Rd (secondary road) and Highway 322. The more pronounced pitch variation on secondary roads results in greater accuracy as compared to highways, when all other factors remain unchanged.

The graph in Figure 6 shows the mean longitudinal position error with respect to the distance update threshold for Rock Road and Highway 322, where the mean error is calculated over a randomly selected 1 km long road segment. The error for Rock Road begins at around .65m but falls to 0.3 m where the error fluctuates by about 0.1 meters until the 80m threshold, where the error increases to .4m. The Highway 322 longitudinal position error remains close to 0.6 m and fluctuates about 0.05 meters to the 85m distance update threshold.

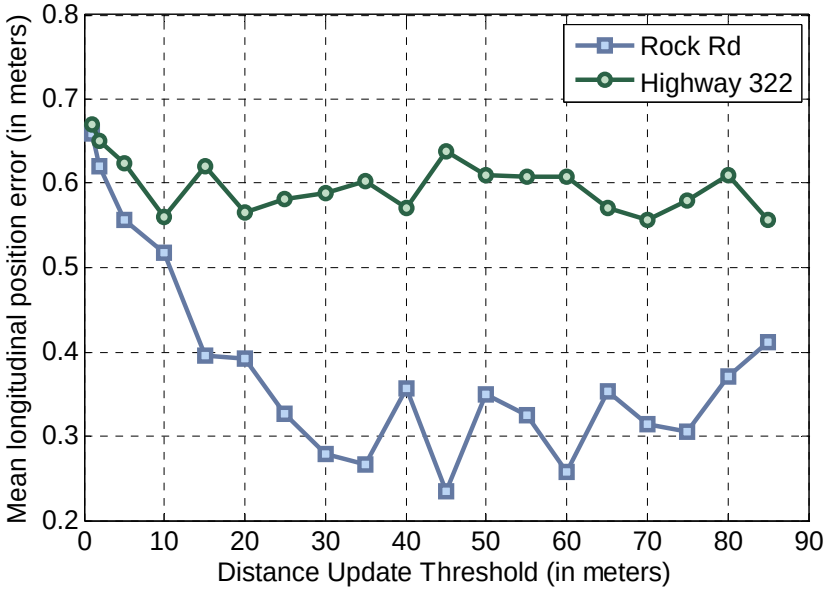

Figure 6: Variation of mean longitudinal position accuracy with varying values of Update Distance Threshold. Mean error calculated over a randomly selected 1 km long road segment.

2.2.3 Field testing of real-time implementation

Since the algorithm and the Simulink model have now been tested offline, the immediate next step in the project is field testing the real-time implementation of the algorithm. Data has already been collected for a typical road intersection and has been post processed. The field test will be held in early November.

2.2.4 Multiple Model Estimation for Road Network Implementation

Once the algorithm is shown to work in real-time, the focus will shift to implementing the algorithm in a more complex and real-life scenario such as when travelling across an intersection. A multiple model estimation scheme will be required for this task, since each road going out from the intersection is represented by a different terrain map, and hence a different model. Literature is being reviewed to identify the most appropriate multiple model estimation scheme for the task.

2.3 Kapsch TrafficCom Inc. Progress

Auburn University has received two DSRC radios. Both radios are installed and interfaced, and preliminary range testing has begun by Auburn.

2.3.1 Initial Range Testing

The DSRC signal strength is measured in Received Signal Strength Indicator (RSSI). The RSSI is an integer ranging from 0 to 100 that is proportional to the power in the received signal. The goal of the initial testing was to find a correlation between the Received Signal Strength Indicator (RSSI) reported by the DSRC radio and range between radios. This correlation could then be used estimate range between radios using the reported RSSI. In order to find a correlation between RSSI and range, both RSSI and range were logged for ranges varying between 1 and 100 meters. The location of the test was on a skid pad located at the NCAT test track in Opelika, Alabama. One DSRC radio was attached to a pole and placed on one end of the skid pad. The other radio was placed in the test vehicle. The antenna for the vehicle-based DSRC radio was located on the back of the roof of the vehicle. Both antennas were placed at approximately the same height above the ground.

In order to get a variety of ranges to use to compare to RSSI, the test vehicle was driven at idling speed both towards and away from the fixed DSRC radio. This data was used to create curve fits for the data. The RSSI was fit to both a 1^{st} and 2^{nd} order quadratic function using least squares. The input to these functions is RSSI and the output is estimated range. There is a noticeable difference in RSSI for when the vehicle is traveling away from the fixed radio as opposed to when the vehicle is traveling towards the fixed radio; therefore, two different sets of 1^{st} and 2^{nd} order curve fits were computed- one for when the vehicle was traveling away from the base radio and one for when the vehicle was traveling towards the base radio.

The graph below shows RSSI a function of distance between radios. The data is split into sets groups. One set of data is for when the test vehicle is traveling away from the base DSRC radio and it is represented by red triangles. The other set of data is for when the test vehicle is traveling towards the base DSRC radio and it is represented by green circles The RSSI is noticeably higher for the case when the vehicle is traveling away from the base radio.

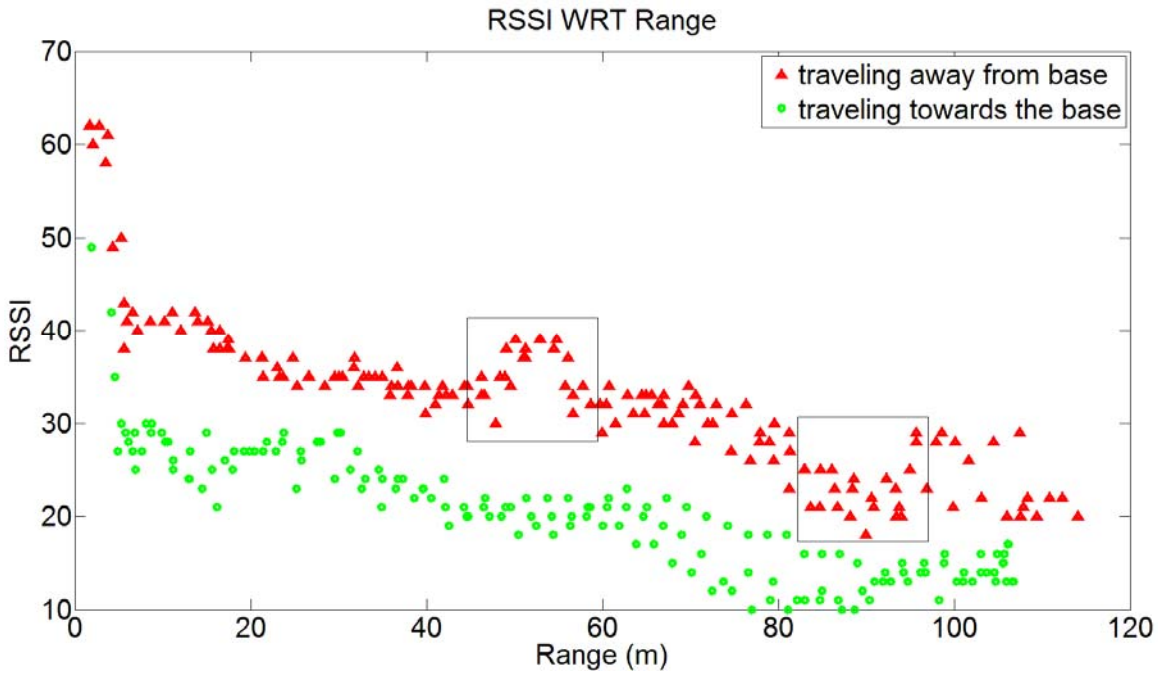

Figure 7: Plot of received signal strength indicator with respect to range between DSRC radios for when the test vehicle is traveling away and towards the base DSRC radio.

When using the curve fits to estimate range using only RSSI, the standard deviation of the error in range is around 15 m^2. The signal strength fluctuates too much to create a strong correlation between range and signal strength. Signal strength could be used to get a general idea of the range between radios; however, range estimates based of signal strength are not accurate enough to incorporate into the current navigation filter.

The results of the experiment show that signal strength varies a great deal with respect to range between radios. One major source of fluctuation is obstructions between radios. Signal strength drops considerably when the signal travels through any solid medium. This can be seen by the difference in signal strength depending on the direction of travel from the base radio. The signal strength is significantly greater when the vehicle is traveling away from the base radio because the line on sight between the radios is clear. When the vehicle is traveling towards the base radio, signal strength is degraded due to the signal passing through the vehicle.

Another source of signal fluctuation is multi-path. Even if the line of sight between antennas is clear, signal strength can be degraded due to multiple copies of the same signal arriving at the antenna. One copy of the signal comes directly from the base DSRC radio. Ideally, this would be the only copy of the signal arriving at the user's radio. Other copies of the original signal come from the signal bouncing off solid surfaces. The signal coming directly from the base radio and the reflected signals are combined at the antenna. The DSRC radio's measure of signal strength comes from the amplitude of the combined signal. If the direct signal and the reflected signal are in phase, then the amplitude of both waves will be added together. This will cause a rise in signal strength. If the direct signal and the reflected signal are out of phase by π radians, then the amplitude of the reflected wave will be subtracted from the amplitude of the

direct wave. This will cause a fall in signal strength. The effect of multi-path can be seen in the boxed in area of Figure 7.

Some of the energy in a reflected signal will be absorbed by the surface it reflects off. The amount of energy absorbed by the surface is dependent on the material of the surface. Paved roads reflect much of the energy in signals that bounce off of it. This causes the reflected signal to have a large amplitude which will cause a large drop in signal strength when the reflected and direct signal are out of phase. Studies have shown that strategic placement of wave absorbers can significantly decrease drops in signal strength due to multi-path. Fluctuation in signal strength due the signal reflecting off the road is most prevalent when range between radios is less than 100 meters. When the range between radios is less than 100 meters, the signal strength follows a Rician fading distribution. Past 100 meters, the signal strength follows a Rayleigh fading distribution. This 100 meter critical distance assumes that the antennas are at the same height.

2.4 Auburn Current Progress

Auburn University has worked extensively with each team member involved in the project, as indicated in their respective sections of the report. Auburn specifically has conducted much of the testing described in the Kapsch current progress section of the report. In addition, Auburn is working on the integrated testing system using the MOOS framework. MOOS is a cross platform network based communications architecture which allows for quick and easy testing and recording of test runs. Auburn has tasked itself with interfacing each of the subsystems (which are not required to interface with MOOS) into the MOOS framework.

3. Future Work

3.1 Sarnoff Future Work

3.1.1 Analysis of Data

The sequences collected at the Auburn test track will be synchronized with the ground truth positioning data and analyzed. This includes assessing the performance with and without IMU, with and without visual landmarks, at different frame rates, and front-only vs. front and back camera sets.

3.1.2 Use of GPS packets

The Sarnoff visual navigation system will use GPS packets that are intermittent and give position but not heading. These packets will be used when available to correct drift and place the output poses in a global coordinate frame.

3.1.3 Delivery of Clevo laptop

The Clevo laptop will be sent to Auburn for running the visual navigation system live, collecting data for offline processing, and calibrating the cameras if necessary.

3.2 Penn State Future Work

Penn State's plans for the near future involve validation of the SPKF algorithm and Simulink model in a real-life environment. This task is expected to be completed in a couple of weeks. Following the completion of this task, Penn State will modify the existing Simulink diagram to include multiple estimators, one for each road connected to an intersection. By the next quarterly report, it is expected that the framework for testing the algorithm at a simulated intersection will be ready.

Concurrently, Penn State will begin looking more closely at approaches for optimizing the algorithm, especially to minimize memory and data transfer requirements. Specifically, Penn State will analyze the effect of using a static buffer during terrain map retrieval as compared to a dynamic buffer. Additionally, Penn State will review existing strategies for storing terrain data to see if memory requirements may be optimized.

3.3 Kapsch Future Work

Kapsch future work includes investigating methods of ranging using message time of flight. A precise measurement of the time from when a radio sends a request for an acknowledgement and when the acknowledgement is received can be used to estimate range between radios. Measuring the two-way time of flight will allow range estimation without syncing each radio's clock. Future work will also include investigating methods of using RSSI to estimate the standard deviation of the range estimate error.

3.4 Auburn Future Work

Auburn will continue aiding each team member with testing and interfacing onto the test vehicle, including interfacing and refinement of the MOOS system. In addition, work involving the Integrated Positioning System (IPS) will begin using simulated measurements from each of the subsystems.

References

[1] Dean, A.; Terrain-based Road Vehicle Localization using Attitude Measurements, Ph.D. Dissertation, The Pennsylvania State University, 2008

[2] Next Generation Vehicle Positioning Techniques for GPS-Degraded Environments to Support Vehicle Safety and Automation Systems, FHWA BAA DTFH61-09-R-00004, Exploratory Advanced research Program, Quarterly Report 1, 2009

[3] Gelb, A. Editor, Applied optimal Estimation, M.I.T. Press, Cambridge, Mass., 1974.

[4] Han, S., Wang, J., and Knight, N.; Using Allan Variance to determine the Calibration Model of Inertial Sensors for GPS/INS Integration, *Proceedings of the 6th International Symposium on Mobile Mapping Technology*, Sao Paulo, Brazil, 2009.

[5] Xing, Z., and Gebre-Egziabher, D.; Modeling and Bounding Low Cost Inertial Sensors, *IEEE/ION Position, Location and Naviagtion Symposium*, 2008.

[6] Wall, J.; A Study of the Effect of Stochastic Inertial Sensor Errors in Dead-Reckoning Navigation, M.S. Thesis, Auburn University, 2007

[7] Miucic, R., Popovic Z., Mahmud, S.; "Experimental Characterization of DSRC Signal Strength Drops," Intelligent Transportation System, 2009. ITSC '09. 12th International IEEE Conference on 4-7 Oct. 2009 Page(s):1-5

[8] Pokharel, R., Toyota, M., Hashimoto, O.; "Analysis on Effectiveness of Wave Absorbers to Improve DSRC Electromagnetic Environment on Express Highway," Microwave Theory and Techniques, IEE Transactions on Sept. 2005 Vol 53 Issue 9 Page(s):2726-2731

[9] Yin, J., Holland, G., ElBatt, T., Fan Bai; Krishnan, H.; "DSRC Channel Fading Analysis From Empirical Measurement," Communications and Networking in China, 2006. ChinaCom '06. First International Conference on 25-27 Oct. 2006 Page(s):1-5

[10] Ferrari, V., Tuytelaars, T., and Van Gool, L.; Object Detection by Contour Segment Networks, *Proceedings of the European Conference on Computer Vision*, 2006

Gantt Chart


2009
2010
October
November
December
January
February
March
April
May
June
July
August
Septembe
Schedule (Proposal)
1.0 Project Management
1.1 Team Meetings
1.2 Conduct Expert Panel Mtgs
2.0 Literature Survey
3.0 Investigate Terrain-Based Localization
3.1 Install on Test Vehicle
3.2 Define Test Protocol
3.3 Collect Characterization Data and Analyze Results
4.0 Investigate Visual Odometry Based Positioning
4.1 Install on Test Vehicle
4.2 Define Test Protocol
4.3 Collect Characterization Data and Analyze Results
5.0 Investigate DSRC-based RF Ranging
5.1 Install DSRC Equipment on Test Vehicle and Test Track
5.2 Define Test Protocol
5.3 Collect Characterization Data and Analyze Results
Milestone 1: Testing and Analysis Completed for Each Positioning Technique
6.0 Define Integrated Positioning System
6.1 Define Initial IPS
Milestone 2: Define Initial Integrated Positioning